09PFL-0507

Combustion Control of Diesel Engines Using Injection Timing

M. Hillion, H. Buhlbuck, and J. Chauvin
IFP, France.

N. Petit
MINES ParisTech, France.

ABSTRACT

We propose a model-based control strategy to adapt the injection settings according to the airpath dynamics of a conventional Diesel engine. This approach complements existing airpath and fuelpath controllers, and aims at accurately controlling the middle of combustion. For that purpose, start of injection is adjusted based on a combustion model and intake manifold conditions. In particular, no in-cylinder sensor is used. Simulation results are presented, which stress the relevance of the approach.

INTRODUCTION

In a Diesel engine, the several phases preceding combustion can be described according to the timeline detailed in Figure 1. There are two main phases corresponding to the airpath subsystem (which involves the intake manifold, the intake throttle, the turbocharger, the Exhaust Gas Recirculation (EGR), and the EGR valve) and the fuelpath subsystem (which consists of the injectors). As these subsystems are clearly independent of each other and act at different times and with different timescales, distinct controllers are usually considered.

Airpath controllers have long been proposed (see [1], [2] and their references). They result in efficient tracking of the intake manifold variables (reference total mass, Burned Gases Rate (BGR[1]), and temperature of the intake charge) even during transients. Usually, three main actuators are employed (EGR valve, intake throttle and turbocharger).

Classic fuelpath controllers can be described as follows. During the cylinder compression phase, fuel is injected and mixed with the compressed air and burned gas mixture. The fuel vaporizes and auto-ignites after the so-called ignition delay (see Figures 1 and 2). Standard fuelpath control strategies focus on controlling injected fuel mass and timing to meet the driver's torque request. These are usually computed by means of a map using as inputs the most influencing variables: the engine speed and the driver's torque demand.

This control structure is sufficient to provide a stable Diesel combustion at steady state. On the other hand, during transient, offsets of the cylinder initial conditions (e.g. pressure, temperature, or composition) shift the combustion phasing. Device ageing and/or clogging (such as the EGR valve and EGR cooler) may also produce unexpected airpath regulation errors resulting in similar combustion phasing shift. The discussed conventional control strategy is in fact non-robust to airpath errors.

[1]Note that in this study, EGR is the system (pipe, valve, and cooler) that permits to recirculate the burned gases, and BGR is the intake (or in-cylinder) variable, ranging from 0 to 1, that represents the rate of burned gases mass.

The Engineering Meetings Board has approved this paper for publication. It has successfully completed SAE's peer review process under the supervision of the session organizer. This process requires a minimum of three (3) reviews by industry experts.

ISSN 0148-7191

In turn, these combustion phasing shifts have impacts on the torque produced and pollutant formation. Figure 3 presents a combustion phasing variation obtained on a four-cylinders Diesel engine, along with its effects on pollutant, noise and torque production. The only parameter which varies during the presented experiment is the injection timing (see Figure 3a). The BGR, intake manifold pressure and temperature, and injected fuel mass are kept constant. These figures clearly show that combustion phasing has a great influence on pollutant, noise and torque production.

Our focus is on developing an improved method capable of achieving the desired transients. To address the discussed issues, i.e. to circumvent changes in the cylinder initial conditions, we propose to use the start of injection (*soi*) as an actuator to control the combustion phasing during BGR, pressure and temperature transients. This is the main contribution of this paper. A noticeable point of our approach is that *this control variable can be used on all commercial line engines without requiring any hardware upgrade*.

In this paper, we assume that the *soc* can be modeled by a Knock Integral Model (KIM) (see [3], [4] or [5]) and that the Rate Of Heat Released (ROHR) during combustion can be modeled by a Chmela's model (see [6]). The phasing of the combustion can be represented by a $\mathrm{CA_y}$ variable, which is the crankangle when y per cent of the total energy contained in the fuel has been released. To guarantee that the $\mathrm{CA_y}$ occurs at a desired setpoint, we update the *soi* according to a first order development of the models.

The paper is organized as follows. First, we detail existing combustion control technologies that we wish to complement and present our approach. After a presentation of the models we base our study on, along with the main physical assumptions underlying our work, we formulate the control problem, and propose a solution at first order. Simulation results are then reported and discussed. Conclusions are given at the end of the paper.

CURRENT COMBUSTION CONTROLLERS AND PROPOSED IMPROVEMENT

A complete nomenclature of engine variables is given in Table 2. In generally observed engine setups, airpath and fuelpath controllers are used to guarantee that engine variables (pressures, temperatures, and injected fuel mass and timing among others) track reference values. These controllers are used in the context of actual vehicle implementation which implies frequent transients due to varying driver torque demands ($\overline{IMEP}$: Indicated Mean Effective Pressure) and engine speed (N_e). In turn, these demands result in frequent transients for reference airpath and fuelpath variables.

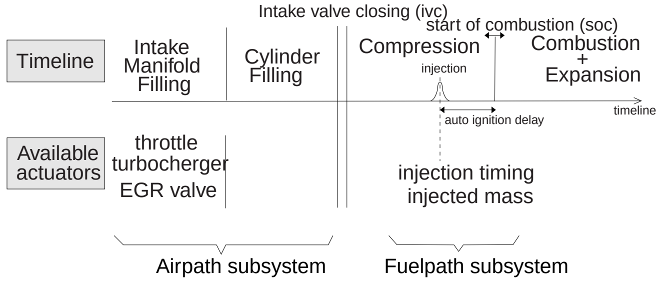

Figure 1: Timeline of Diesel engine cycle with direct injection

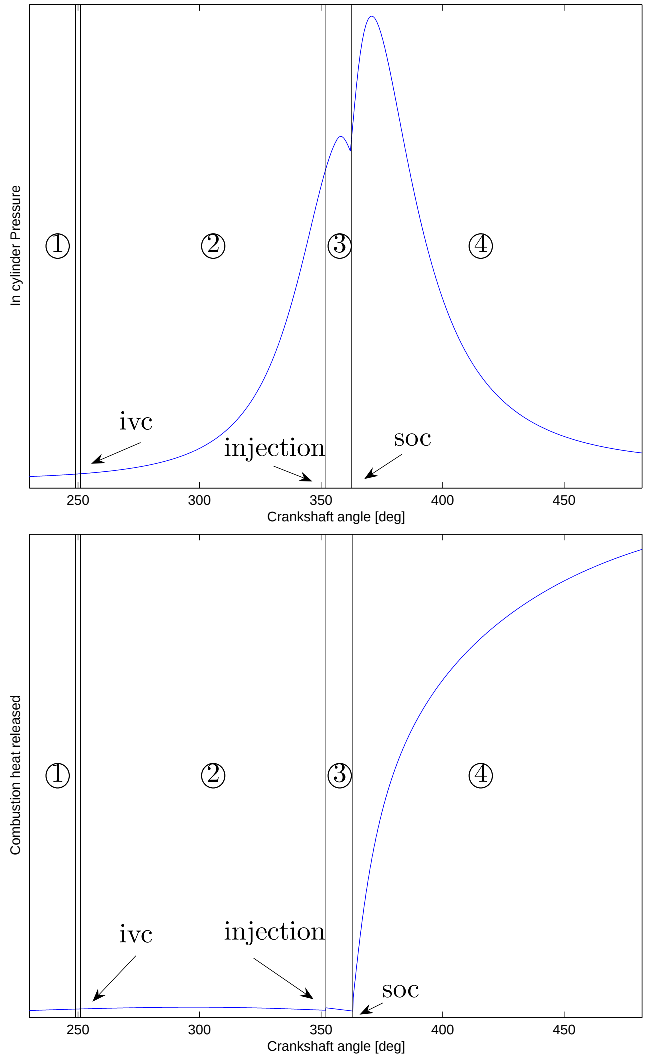

Figure 2: Experimental results: in-cylinder pressure and combustion heat released during one cycle ($N_e = 1500rpm$, $IMEP = 6bar$): ① filling the cylinder, ②: compression, ③: auto ignition, ④: Combustion and expansion, *ivc*: intake valve closing, *soc*: start of combustion. (360 corresponds to the Top Dead Center)

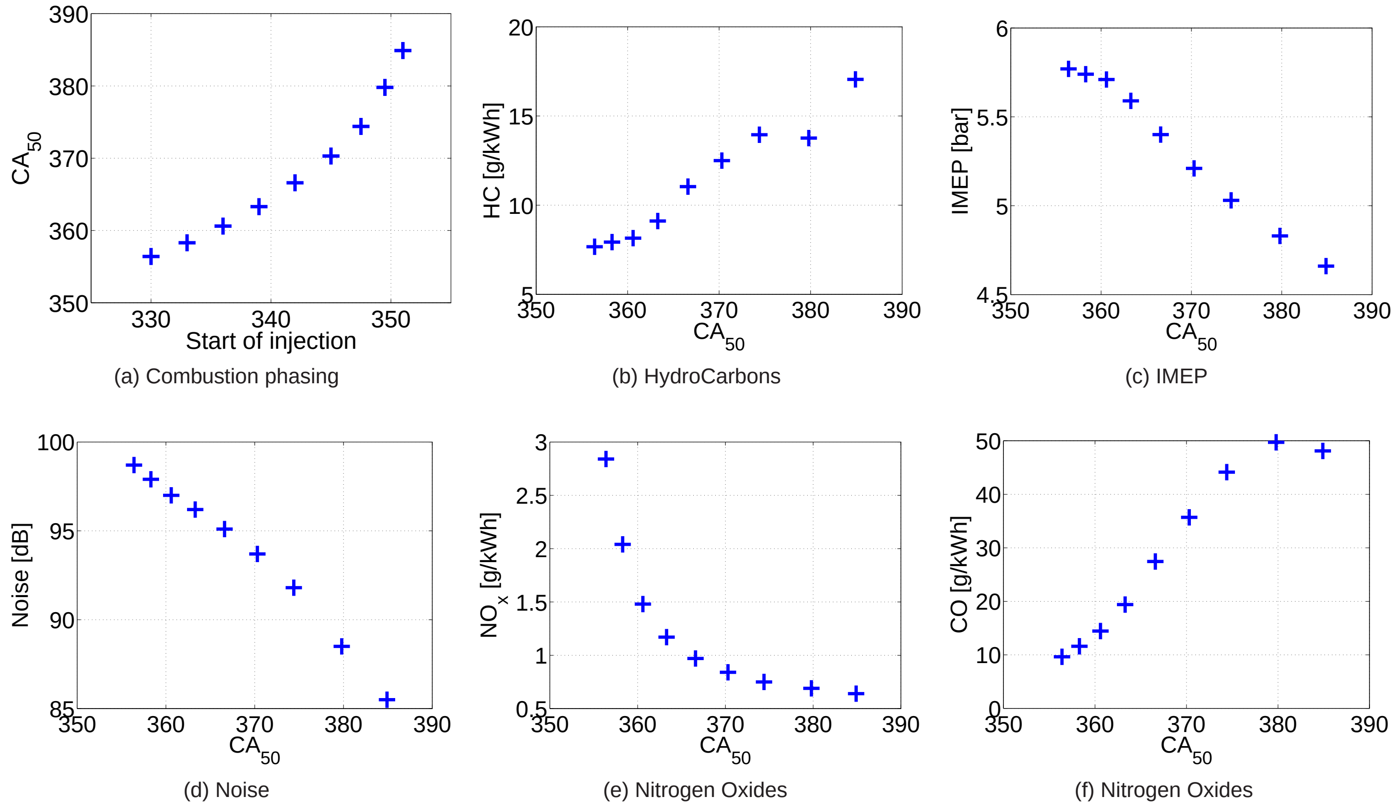

(a) Combustion phasing (b) HydroCarbons (c) IMEP

(d) Noise (e) Nitrogen Oxides (f) Nitrogen Oxides

Figure 3: Experimental results obtained on a four-cylinders Diesel Engine: influence of the combustion phasing on engine pollutant, noise and torque production. The combustion phasings are obtained through off-line in-cylinder pressure analysis. The pollutant magnitudes are obtained through exhaust gases analysis.

Table 1: Acronyms

ROHR	Rate of Heat Released
$\mathrm{CA_y}$	y% of Mass Fuel Burnt
soc	Start Of Combustion
soi	Start Of Injection
ivc	Intake Valve Closing
EGR	Exhaust Gas Recirculation (system)
BGR	Burned Gas Rate
KIM	Knock Integral Model
TDC	Top Dead Center
VCR	Variation Compression Ratio
VVT	Variable Valve Timing

In closed loop, the airpath subsystem cannot be rendered arbitrarily fast. The culprits are the turbocharger inertia and recirculation hold-ups. On the other hand, injection parameters can be changed from one cycle to the next one. Neglecting fuelpath transients, classic fuelpath controllers set injection parameters instantaneously to values corresponding to the targeted steady states $((\overline{\theta}_{soi}, \overline{m}_{inj}) = f(\overline{IMEP}, Ne))$. This strategy leads to large overshoots or undershoots of the combustion phasing during transients (see [7] for more details) which directly impacts the produced torque or pollutant formation (see Figure 3).

POSSIBLE UPGRADES FROM THE LITERATURE

The phasing of the combustion is known to have a direct impact on the produced torque and on the pollutant formation. Controlling the combustion phasing ($\mathrm{CA_y}$) appears as a natural answer to the exposed transient problems. We now sketch an overview of the literature on this subject.

In [8], Haraldsson *et al.* present closed-loop combustion control using Variable Compression Ratio (VCR) as actuator. Changing the compression ratio directly impacts on the rise of pressure and temperature in the cylinder during compression, making differences in thermodynamic conditions during auto ignition and combustion. This is then used to control the $\mathrm{CA_{50}}$.

In [9], Olsson *et al.* present a dual-fuel solution. These two fuels have different auto-ignition properties. Taking advantage of this inequality, $\mathrm{CA_{50}}$ can be regulated by changing the recipe of the mixture to be injected.

In [10], [11], and [12] the authors present Homogeneous Combustion Compression Ignition (HCCI) control results based on a Variable Valve Timing (VVT) actuation, which allows to trap hot exhaust gases in the cylinder from one cycle to the next. The charge temperature can thus be modified. The whole combustion process is then delayed or advanced.

Table 2: Nomenclature

Symb.	Engine Variables	Unit
θ	Crankshaft angle	deg
$V(\theta)$	Cylinder volume	m^3
$P(\theta)$	Cylinder pressure	Pa
$T(\theta)$	Cylinder temperature	K
X	In-cylinder burned gas rate (BGR)	-
ϕ	equivalence ratio	-
V_{ivc}	In-cylinder volume at *ivc*	m^3
P_{ivc}	In-cylinder pressure at *ivc*	Pa
T_{ivc}	In-cylinder temperature at *ivc*	K
M_{ivc}	In-cylinder gases mass at *ivc*	kg
V_{cyl}	Displaced volume	m^3
P_{int}	Intake manifold pressure	Pa
T_{int}	Intake manifold temperature	K
θ_{soi}	Crankshaft angle of the *soc*	deg
θ_{soc}	Crankshaft angle of the *soc*	deg
D_{fuel}	Fuel injection mass flow	kg/s
m_{inj}	Injected fuel mass per stroke	kg/str
M_f	fuel mass already injected (ranges from 0 to m_{inj})	kg
k	turbulent kinetic energy	J
Q	Combustion Heat released	J
Q_{LHV}	Fuel low heating value	J/kg
γ	Ratio of specific heats	-
$h(X)$	Impact of the BGR on combustion	-
η_{vol}	Volumetric efficiency	-
$IMEP$	Indicated Mean Effective Pressure	bar
N_e	Engine speed	rpm

PROPOSED UPGRADE All the controllers presented in the previous section use high frequency in-cylinder sensors and/or additional actuators (VCR, dual-fuel system, VVT). Such solutions provide accurate closed loop control solution at the expense of costly hardware upgrades (see [13]). Rather, to control the $\mathrm{CA_y}$, we propose a solution requiring only standard devices which are available on all commercial-line engines. *A main advantage of our method is that it does not require cylinder pressure sensors*.

Consider the fuelpath subsystem whose dynamic response, as previously discussed, is inconsistent with the dynamic response of the airpath subsystem. This subsystem is controlled by the fuel injection. The injected mass is used to produce a reference torque and it cannot be changed without jeopardizing performance. Therefore, only one degree of freedom of the fuelpath remains as possible additional control variable. It is the *soi* which is pictured in the combustion timeline in Figure 1.

In [14], Vigild *et al.* propose a *soi* adaptation to the intake manifold conditions based on look-up tables. This strategy results in a much better HCCI combustion stability but requires a tedious calibration effort to construct correction maps.

In [15], we presented a control strategy based on a feed forward *soi* correction. The controller aimed at keeping the start of combustion at its reference value. This approach is extended to the control of any combustion timing variables.

In our approach, we propose to cascade the control of the $\mathrm{CA_y}$ onto the *soi* (θ_{soi}) variable. This implies that, instead of constant values corresponding to references, θ_{soi} has non-constant values during transients. Our control strategy is based on an ignition delay model and a combustion model; thus, *does not need any in-cylinder sensors*. It is in fact open loop. These models involve physical parameters of the gases aspirated in the combustion chamber (i.e. BGR, temperature, pressure, air/fuel ratio, turbulence) and parameters of the fuel injection (i.e. *soi*, injected fuel mass).

MODELING

Our control strategy aims at controlling the $\mathrm{CA_y}$ with a model-based feed forward controller. Thus, we need a model of the processes taking place between the *soi* and the desired $\mathrm{CA_y}$. These are the ignition delay and the combustion.

The fuel injection does not directly initiate the combustion (this is rather different from the spark advance technology in spark ignited engines). In fact, combustion occurs after the ignition delay (defined as the lag between *soi* and *soc*). Physical and chemical processes must take place before combustion starts. The physical processes are the vaporisation of the fuel followed by its mixing with the air/burned-gases charge. Chemical processes are the pre-combustion reactions which do not release significant energy but lead to the auto ignition of the fuel/air/burned gases mixture. This delay depends on the physical conditions of the mixture (pressure, temperature, composition, fuel/air ratio) (see [5]).

Combustion starts after ignition delay. The rate of heat release (ROHR) also depends on the physical conditions of the mixture such as the air/fuel ratio and on other parameters such as available turbulent kinetic energy (see [16] or [6]).

In this section, we present both models along with the assumptions made throughout the control strategy development.

AUTO IGNITION MODELLING

The Knock Integral Model - Many models have been proposed in the literature, depending on the engine, the fuel and/or the working conditions. However, all these models are expressed under the KIM originally proposed in [4]. This model gives an implicit relation among θ_{soi}, θ_{soc} and the physical in-cylinder parameters such as $P(\theta)$, $T(\theta)$, X, and equivalence ratio ϕ under the following integral form

$$\int_{\theta_{soi}}^{\theta_{soc}} \frac{\mathcal{A}^{ai}(p(\theta))}{N_e} d\theta \quad = \quad 1 \tag{1}$$

where $\mathcal{A}^{ai}$ is an Arrhenius function, and $p(\theta)$ is a vector of in-cylinder physical properties. In [16], Barba *et al.* adapted a phenomenological model for conventional Diesel applications

$$\begin{aligned} p(\theta) &= (P(\theta), T(\theta), \phi) \\ \mathcal{A}^{ai}(p(\theta)) &= c_1 \phi^{c_2} \left(\frac{P(\theta)}{P_{ref}}\right)^{c_3} \exp\left(-\frac{T_A}{T(\theta)}\right) \end{aligned} \tag{2}$$

where c_1, c_2, c_3, P_{ref}, and T_A are constant parameters. In [3], Swan *et al.* use the following Arrhenius function

$$\begin{aligned} p(\theta) &= (P(\theta), T(\theta), X, \phi) \\ \mathcal{A}^{ai}(p(\theta)) &= \frac{\phi^x}{(C_1 + C_2 X)\exp(bP(\theta)^n / T(\theta))} \end{aligned} \tag{3}$$

where x, C_1, C_2, b and n are constant parameters. In [17], Lafossas *et al.* extend the KIM to large burned gases rates. The proposed model is thus suitable for HCCI combustion

$$\begin{aligned} p(\theta) &= (P(\theta), T(\theta), X)^T \\ \mathcal{A}^{ai}(p(\theta)) &= \frac{A}{1 + CX} P(\theta)^n \exp\left(-\frac{T_A}{T(\theta)}\right) \end{aligned} \tag{4}$$

where A, C, n, and T_A are constant positive parameters. Model 4 is used in the current study, but the proposed control strategy can be used with the Models 2, 3 or any other (smooth) function $\mathcal{A}^{ai}$.

Relating the KIM to Available Measurements - The proposed Model 1 is expressed in terms of in-cylinder thermodynamics quantities ($P(\theta)$, $T(\theta)$, and X) which are not directly measured on commercial line engines. Therefore, we rewrite it in terms of different parameters. To compute the in-cylinder pressure ($P(\theta)$) and in-cylinder temperature ($T(\theta)$) during compression, we assume that a static relation holds. In particular, the transformation is considered isentropic. Classically, during this isentropic transformation, PV^γ and $TV^{\gamma-1}$ are both constant. In these relations, V represents the cylinder volume, which is known as a function of the crankshaft angle θ. This thermodynamic assumption (see e.g. [18]) is supported by the fact that, during the compression stroke, gas temperature is much lower than during the combustion stroke. In short, during the compression stroke, wall heat losses are neglected.

We consider the *ivc* (intake valve closing) as initial time for the isentropic transformation.These considerations yield to

$$P(\theta) = P_{ivc} v_{ivc}(\theta)^\gamma \tag{5}$$

$$T(\theta) = T_{ivc} v_{ivc}(\theta)^{\gamma-1} \tag{6}$$

$$\text{with} \quad v_{ivc}(\theta) \triangleq \frac{V(\theta_{ivc})}{V(\theta)}$$

The cylinder pressure at *ivc*is assumed to equal the intake manifold pressure right before the *ivc*. This pressure is measured. This assumption is supported by the fact that the pressure equilibrium is reached at the *ivc*between the intake manifold and the cylinder. The cylinder temperature at *ivc*is reconstructed from the intake manifold temperature (measured) and the volumetric efficiency (usually mapped through table look-up) via the ideal gas law (in the following equation M_{ivc} is the trapped gas mass in the cylinder)

$$\left\{ \begin{array}{rcl} P_{ivc} &=& P_{int} \\ \eta_{vol} &=& M_{ivc} \frac{RT_{int}}{P_{int} V_{cyl}} \\ M_{ivc} &=& \frac{P_{ivc} V_{ivc}}{RT_{ivc}} \end{array} \right. \Rightarrow \left\{ \begin{array}{rcl} P_{ivc} &=& P_{int} \\ T_{ivc} &=& \frac{V_{ivc}}{V_{cyl}} \frac{T_{int}}{\eta_{vol}} \end{array} \right. \tag{7}$$

Finally, in (1), X is assumed to be constant from the *ivc*to the *soc*. This is not unrealistic, because there is no chemical reaction taking place between *ivc*and *soc*. Eventually, the burned gases rate X in the cylinder is supposed equal to the intake manifold burned gases rate obtained from an observer presented in [1].

One can notice that we do not take into account residuals in-cylinder gases in the estimation of T_{ivc} and X. Slight errors are thus made on the estimation of the real in-cylinder conditions.

The model used throughout this paper is Model 4 which do not depend on ϕ. In the event this variability should be considered, the assumptions made on X can be transposed on ϕ.

By substituting Equations (5) and (6) into (1), the auto ignition model takes the form

$$\int_{\theta_{soi}}^{\theta_{soc}} \frac{\mathcal{A}_{ivc}^{ai}(p_{ivc},\theta)}{N_e} d\theta = 1 \tag{8}$$

$$\text{with} \quad p_{ivc} \triangleq p(\theta_{ivc})$$
$$\mathcal{A}_{ivc}^{ai}(p_{ivc},\theta) \triangleq \mathcal{A}^{ai}(p(\theta))$$

Equation (8) summarizes the influence of the physical parameters values at *ivc*on the start of combustion. In particular, Equation (4) becomes

$$\begin{aligned} p_{ivc} &= (P_{ivc}, T_{ivc}, X) \\ \mathcal{A}_{ivc}^{ai}(p_{ivc},\theta) &= \\ & \frac{A}{1+CX} {P_{ivc}}^{n} v_{ivc}(\theta)^{n\gamma} \exp\left(-\frac{T_A}{T_{ivc} v_{ivc}(\theta)^{\gamma-1}}\right) \end{aligned} \tag{9}$$

In the current study, we make the classical assumption that the engine speed N_e is constant during the ignition period (see Equation (8)).

HEAT RELEASE MODEL

Chmela's model - The ROHR is modeled with a Chmela's combustion model originally proposed in [6]. This model takes into account the main phenomena influencing the rate of released heat, namely the available fuel in the chamber (M_f) and the turbulent kinetic energy (k). This model has the following shape

$$\frac{dQ}{d\theta} = C_{mode}(M_f(\theta) - \frac{Q}{Q_{LHV}}) e^{C_{rate} \frac{\sqrt{k(\theta)}}{\sqrt[3]{V(\theta)}}} h(X) \tag{10}$$

where

- M_f is the fuel mass available for combustion (that is the fuel already injected).
- k is the local turbulent kinetic energy.
- $h(X)$ is an adaptation of the classical Chmela's model to take into account the presence of burned gases in the cylinder. The proposed strategy does not depend on the particular shape of h. The presented results are obtained with the function $h(X) = (1-X)^{\beta}$.
- C_{mode}, C_{rate} and β are constant calibration parameters of the model.
- Q_{LHV} is the low heating value of the considered fuel.

In Direct injection Diesel engines, turbulent kinetic energy mainly arises from the fuel jets (see [6]). This energy dissipates into the cylinder with a time constant C_{diss}. Finally, following [6], the turbulent kinetic energy density k is governed by the equation.

$$\frac{dk}{d\theta} = -\frac{C_{diss}}{6N_e} k + \frac{C_d}{M_{ivc} N_e} D_{fuel}(\theta)^3 \tag{11}$$

where

- D_{fuel} is the fuel injection mass flow.
- M_{ivc} is the in-cylinder gases mass (including fresh air and burned gases).
- C_d, C_{diss} are constant calibration parameter of the model.

Towards an integral model - To design our control law, we make the following assumptions on the fuel injected mass flow

1. Assumption 1: the fuel injection is over when the combustion begins. Define Δ_{inj} as the duration of the injection. We have $\theta_{soi} + \Delta_{inj} < \theta_{soc}$.
2. Assumption 2: the fuel injection mass flow depends on the injected fuel mass (pattern of the flow mass) and the start of injection (location of the pattern in time). In particular, shifting the start of injection in time only shifts the pattern without modifying it.

These assumptions are pictured in Figure 4. They lead to consider D_{fuel} as a function $D_{fuel}(m_{inj}, \frac{\theta - \theta_{soi}}{N_e})$ Fur-

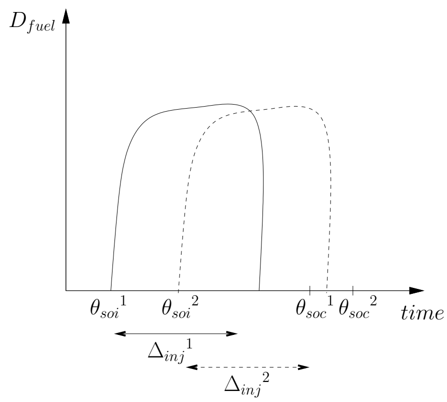

Figure 4: Fuel injection flow mass pattern for two different injection timing

ther, these assumptions permit to transform the ROHR model under an integral form. First, we analytically determine the turbulent kinetic energy density k as the solution of the linear first order differential Equation (11)

$$k(\theta) = C_d e^{-\frac{C_{diss}}{6N_e}(\theta - \theta_{soi})} \frac{k_0(\theta)}{M_{ivc}} \tag{12}$$

where

$$k_0(\theta) = \int_{\theta_{soi}}^{\theta} D_{fuel}(m_{inj}, \frac{z-\theta_{soi}}{N_e})^3 e^{\frac{C_{diss}}{6N_e}(z-\theta_{soi})} \frac{dz}{N_e} \quad (13)$$

As the ROHR model describes the combustion, we only want to use it after the start of combustion. Following the assumption 1, $\theta > \theta_{soc} > \theta_{soi} + \Delta_{inj}$ in (13). Secondly, following assumption 2, the integrand of the Equation (13) vanishes outside $[\theta_{soi}, \theta_{soi} + \Delta_{inj}]$. Finally, using the substitution $u = z - \theta_{soi}$ we obtain the following expression for k_0

$$k_0(\theta) = k_0 = \int_0^{\Delta_{inj}} D_{fuel}(m_{inj}, u)^3 e^{\frac{C_{diss}}{6N}(u)} \frac{du}{N_e} \quad (14)$$

This stress that k_0 solely depends on the shape of the injection pattern D_{fuel}. In particular it does not depend on the start of injection or crankshaft angle.

Equation (10) presents a general heat release model. Using the assumption 1, the fuel mass available during combustion ($M_f(\theta)$) equals the injected fuel mass per cycle (m_{inj}). We denote x the burned fuel mass fraction. Using the classical relation (see [5]) $Q = x m_{inj} Q_{LHV}$ we have

$$\begin{aligned} & \frac{dx}{d\theta} = \frac{C_{mode}}{Q_{LHV}}(1-x) e^{C_{rate}\frac{\sqrt{k(\theta)}}{\sqrt[3]{V(\theta)}}} h(X) \\ \Leftrightarrow \quad & \frac{dx}{1-x} = \frac{C_{mode}}{Q_{LHV}} e^{C_{rate}\frac{\sqrt{k(\theta)}}{\sqrt[3]{V(\theta)}}} h(X) d\theta \\ \Leftrightarrow \quad & \int_0^{\frac{y}{100}} \frac{dx}{1-x} = \int_{\theta_{soc}}^{\mathrm{CA_y}} \frac{C_{mode}}{Q_{LHV}} h(X) e^{C_{rate}\frac{\sqrt{k(\theta)}}{\sqrt[3]{V(\theta)}}} d\theta \end{aligned}$$

Once $y \in [0, 100]$ is chosen, the previous equation gives an integral form of the Chmela's model

$$g(y) = \int_{\theta_{soc}}^{\mathrm{CA_y}} \mathcal{C}(m_{inj}, X, \theta_{soi}, M_{ivc}, \theta) d\theta \quad (15)$$

where

$$\mathcal{C}(m_{inj}, X, \theta_{soi}, M_{ivc}, \theta) = \frac{C_{mode}}{Q_{LHV}} h(X) e^{C_{rate}\frac{\sqrt{k(\theta, \theta_{soi}, m_{inj}, M_{ivc})}}{\sqrt[3]{V(\theta)}}} \quad (16)$$

$$g(y) = \int_0^{\frac{y}{100}} \frac{dx}{1-x} = \ln \frac{100}{100-y}$$

At the beginning of the modeling Section, a vector of in-cylinder parameter has been introduced to gather all in-cylinder thermodynamic variables of interest (see Equation (1)). Without any loss of generality, we include M_{ivc} in this vector so that Equation (15) becomes

$$g(y) = \int_{\theta_{soc}}^{\mathrm{CA_y}} \mathcal{C}_{ivc}(m_{inj}, \theta_{soi}, p_{ivc}, \theta) d\theta \quad (17)$$

with

$$\mathcal{C}_{ivc}(m_{inj}, \theta_{soi}, p_{ivc}, \theta) = \frac{C_{mode}}{Q_{LHV}} h(X) e^{C_{rate}\frac{\sqrt{k(\theta, \theta_{soi}, m_{inj}, M_{ivc})}}{\sqrt[3]{V(\theta)}}} \quad (18)$$

CONTROL PROBLEM

At steady state, all the $p_{ivc} \triangleq (P_{ivc}, T_{ivc}, X, M_{ivc})$ parameters are stabilized by the airpath controller to their reference values ($\overline{p}_{ivc}$). Further, the injection timing θ_{soi} is directly set to its reference value ($\overline{\theta}_{soi}$) by the fuel-path controller. A reference combustion takes place. All these reference parameters have been optimized together to reach driver's demands and pollutant restrictions.

During transient, due to the non instantaneous airpath dynamic, $\delta p \triangleq p_{ivc} - \overline{p}_{ivc} \neq 0_{\mathbb{R}^3}$. If fuel is injected at the reference time $\overline{\theta}_{soi}$, then $\mathrm{CA_y}$ differs from the reference combustion one (because both $\mathcal{A}_{ivc}^{ai}$ and $\mathcal{C}_{ivc}$ depend on p_{ivc}). We propose to compensate any such known error δp with a corrective offset $\delta\theta_{soi}$ on the injection time reference $\overline{\theta}_{soi}$ so that the actual $\mathrm{CA_y}$ is always equal to $\overline{\mathrm{CA}}_{\mathrm{y}}$.

SOLUTION AT FIRST ORDER

It might be difficult to find an explicit solution to the control problem presented in the previous section when considering models with an integral form (8),(17). A simple way to proceed is to look for an approximate solution. We follow the procedure exposed in [7] to obtain two first order equations, one for Equation (8), and one for Equation (17). We thus obtain from Equation (8)

$$\alpha_{soc}\delta\theta_{soc} + \alpha_{soi}\delta\theta_{soi} + \alpha_p \delta p = 0 \quad (19)$$

with

$$\begin{aligned} \alpha_{soc} &= -\mathcal{A}_{ivc}^{ai}(\overline{p}_{ivc}, \overline{\theta}_{soc}) \\ \alpha_{soi} &= \mathcal{A}_{ivc}^{ai}(\overline{p}_{ivc}, \overline{\theta}_{soi}) \\ \alpha_p &= \int_{\overline{\theta}_{soi}}^{\overline{\theta}_{soc}} \frac{\partial \mathcal{A}_{ivc}^{ai}}{\partial p_{ivc}}(\overline{p}_{ivc}, \theta) d\theta \end{aligned}$$

and from Equation (17)

$$\beta_{CA}\delta\mathrm{CA_y} + \beta_{soc}\delta\theta_{soc} + \beta_{soi}\delta\theta_{soi} + \beta_p\delta p = 0 \quad (20)$$

with

$$\begin{aligned} \beta_{soc} &= \mathcal{C}_{ivc}(\overline{p}_{ivc}, \overline{\theta}_{soc}) \\ \beta_{CA} &= -\mathcal{C}_{ivc}(\overline{p}_{ivc}, \overline{\mathrm{CA}}_{\mathrm{y}}) \\ \beta_{soi} &= \int_{\overline{\theta}_{soi}}^{\overline{\theta}_{soc}} \frac{\partial \mathcal{C}_{ivc}}{\partial \theta_{soi}}(m_{inj}, \overline{\theta}_{soi}, \overline{p}_{ivc}, \theta) d\theta \\ \beta_p &= \int_{\overline{\theta}_{soi}}^{\overline{\theta}_{soc}} \frac{\partial \mathcal{C}_{ivc}}{\partial p_{ivc}}(m_{inj}, \overline{\theta}_{soi}, \overline{p}_{ivc}, \theta) d\theta \end{aligned}$$

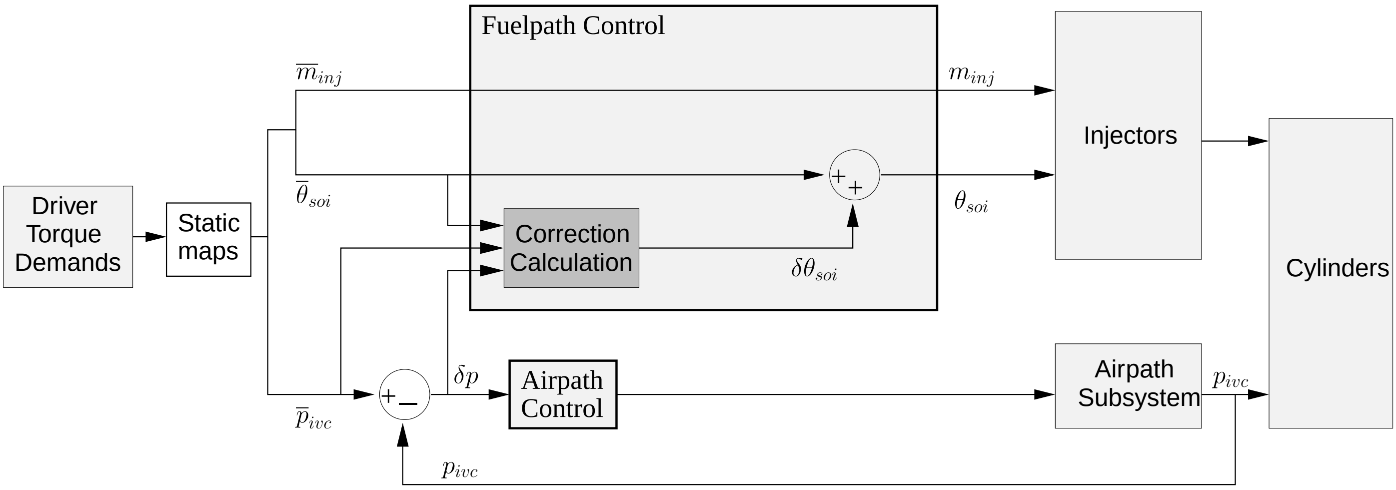

Figure 5: Design of the new control strategy. The dark grey block has been added, counterbalancing airpath errors δp with an *soi* offset.

We want to make $\delta \mathrm{CA_y}$ vanish at all time. Eliminating $\delta\theta_{soc}$ in Equations (19) and (20) gives the desired correction $\delta\theta_{soi}$

$$\delta\theta_{soi} = -\frac{\alpha_{soc}\beta_p + \alpha_p\beta_{soc}}{\alpha_{soi}\beta_{soc} + \alpha_{soc}\beta_{soi}} dp \qquad (21)$$

In practice, this correction is easily computable in real-time, because $\mathcal{A}^{ai}_{ivc}$ and $\mathcal{C}_{ivc}$ are known functions, $\overline{p}_{ivc}$ are the airpath setpoints values, δp are the airpath errors (differences between measured or observed values and their setpoints), $\overline{\theta}_{soi}$ is the reference *soi*, and $\overline{\theta}_{soc}$ and $\overline{\mathrm{CA_y}}$ can be calculated online using the KIM.

SIMULATION RESULTS

SIMULATION SETUP The proposed strategy has been validated on the simulation software AMESim [19]. The combustion model used in the simulator has been validated for engine control purposes in [20]. Basically, this simulation model is almost the same as the one used to obtain the proposed controller. In fact, wall heat losses are now taken into account. A Diesel engine is considered. Its main characteristics are summarized in Table 3.

CONTROLLER DESIGN The general control scheme is presented in Figure 5. It includes the strategy proposed in this paper to control the $\mathrm{CA_y}$. This new strategy is included in the dark-grey module “correction calculation" which implements Equation (21). In this setup, the start of injection θ_{soi} is not simply set to its reference value $\overline{\theta}_{soi}$ but is corrected according to the airpath errors δp. In this section, y has been chosen to be 50, i.e. the proposed controller controls the middle of combustion.

Again, one can remark that this fuelpath strategy *does not need* in-cylinder pressure sensors feedback.

RESULTS The results obtained with the proposed controller are presented at the light of robustness of the combustion phasing towards airpath error. More precisely, we look into the domain of admissible airpath errors such that the $\mathrm{CA_y}$ does no deviate from its reference value more than 1.5 crankangle degrees. In the following of the paper, this domain is denoted by "acceptable domain". The larger the acceptable domain, the more robust the combustion control towards airpath errors is.

The domain of stability has the dimension of the vector of considered airpath errors (p_{ivc}). However, it would be a physical non sense to consider independent variations of P_{ivc}, T_{ivc} and M_{ivc}. These are in fact related through the ideal gas relation. Eventually p_{ivc} is a 4 dimensional, vector depending on 3 independent parameters (P_{int}, T_{int}, and X_{int}).

Table 3: Engine setup used in the simulation

Bore $\times$ Stroke	87.0 $\times$ 92.0 mm
Number of cylinders	4
Compression ratio	14.0:1
Displacement	2.2 Liters
Injection device	Solenoid
Maximum injection pressure	1600 bar
Piston bowl design	$\mathrm{NADI}^{\mathrm{TM}}$
Intake Valve Closing	$\theta_{ivc} = 232$deg
	(360 is Top Dead Center)

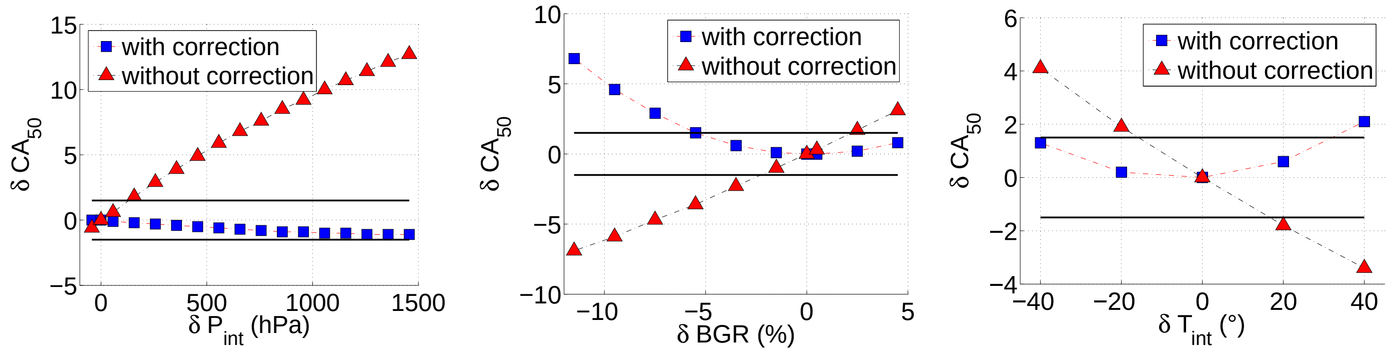

(a) Intake Manifold Pressure (b) Intake Manifold Burned Gas Rate (c) Intake Manifold Temperature

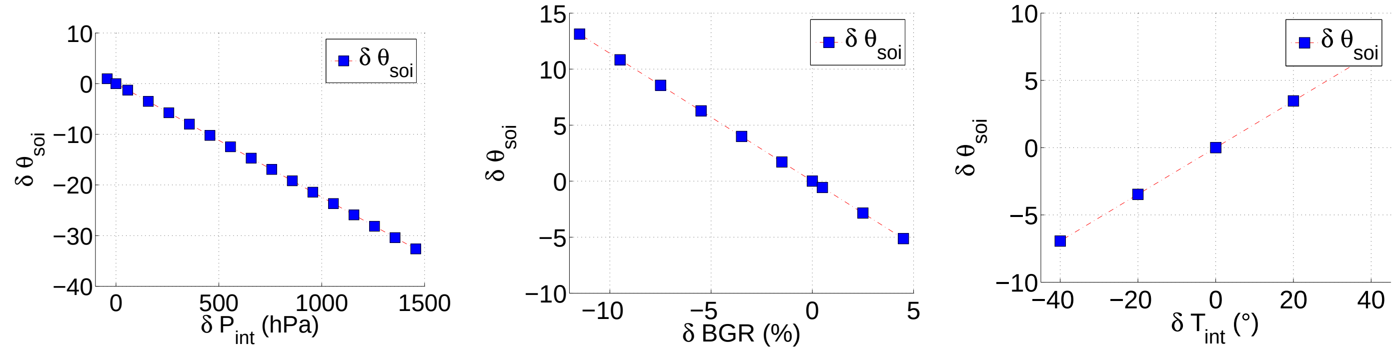

(d) Correction for Intake Manifold Pressure error (e) Correction for Intake Manifold Burned Gas Rate error (f) Correction for Intake Manifold Temperature error

Figure 6: Simulation results (1500rpm, IMEP=3 bar). Intake manifold variations around optimal values with and without correction, impact on the CA_{50} and the corresponding *soi* correction.

Table 4: Acceptable Domain

	Without Corr.	With Corr.
δP_{int}(hPa)	[-40,130]	[-40,1500]
δX_{int}(-)	[-2%,2%]	[-5%,5%]
δT_{int}(°)	[-16,17]	[-40,31]

Independently, and one by one, the three parameters are varied. This procedure yields estimation of the size of the admissible domain. Values are reported in Table 4 (e.g. for nominal values of X_{int} and T_{int}, the pressure P_{int} can be changed within [-40, 1500] without causing too large errors on the $\mathrm{CA_y}$ by the mean of the proposed methodology). More precisely, in Figure 6, the results of variations around reference values of the intake manifold conditions at (1500rpm, IMEP=3bar) are reported. In each figure, the resulting error on the middle of combustion phasing can be compared against the maximum errors according to the criterion (horizontal black line). The acceptable domain has been enlarged for the three intake manifold thermodynamical conditions. In particular, the acceptable domains for intake manifold pressure and temperature have been extended to the overall intake manifold pressure and temperature range of the studied engine (approx. [1010 hPa,2500 hPa] and [20°C,100°C]). The overall BGR domain of the studied Diesel engine is [0,18%]. At this working point, the proposed controller makes the engine controller robust towards intake manifold temperature and pressure errors and considerably extends the domain of acceptable BGR error.

In Figures 7, 8, 9, 10, and 11, we present results obtained for a more global working range of the engine. At each engine speed 800 (Figure 7), 1000 (Figure 8), 1500 (Figure 9), 2000 (Figure 10), and 2500 (Figure 11), we present the acceptable domain for each intake manifold thermodynamical conditions. In these figures, the black line represents the reference value of the considered intake parameter. The red interval and the blue interval picture the acceptable domain (as previously defined) without and with the proposed controller, respectively. In these figures, it clearly appears that the domains of acceptable intake manifold pressure and temperature are considerably enlarged on the entire operating range. Robustness towards these conditions has thus been improved. Yet, two zones in the BGR variations figures are worth mentioning. At low load, the acceptable BGR domain is extended by the proposed control. At higher load, the *soi* correction has the opposite influence. The acceptable domain is smaller than without the correction. We now give an insight into this phenomena.

At low load, little fuel mass is injected into the cylinder so that the injection time (Δ_{inj}) is small enough to consider the assumption 1 as valid. As the load increases, the injected fuel mass increases and the assumption is not valid any more. In particular, the expression (14) of k_0 becomes inaccurate. This has a great impacts on the computed correction (Equation 21). This is particularly visible on the BGR results. In fact, while pressure and temperature errors have an inverse influence on ignition delay and on combustion (for instance, when the pressure is increased, the ignition delay is shortened but the aspirated air mass and then the turbulence is decreased, which in turn slows down the combustion), BGR error has the same impact on ignition delay and on combustion (for instance, it slows down both phenomena when BGR is too high). This is why the inaccuracy of (14) is underlined when the BGR varies significantly.

CONCLUSION AND FUTURE WORK

An improvement for the fuelpath control strategy of Diesel engine has been presented. Instead of directly setting *soi* to its reference value, we propose to adapt the fuel injection settings according to the intake manifold conditions. This controller is based on the linearization of an auto ignition delay model (KIM) and a combustion model. The advantages of the proposed method are

- The *soi* correction is computed from a physical model and does not need any additional calibration. The only calibration is the one of the physical models.
- The *soi* correction is computed using standard engine measurements and does not require in-cylinder pressure sensors.

The presented simulation results stress the relevance of this approach and are very encouraging. The correction permits to increase the robustness of the overall control system to airpath regulation errors. One can expect that this system would easily handle EGR valve clogging or regulation errors, which would usually yield some malicious combustion phasing shift. Some issues related to the implementation of the computations and their possible speed-up remain to be explored. This is the subject of actual research.

This method is very general and can be applied to a very large scope of engine architectures. In particular, it is completely independent of the airpath architecture (low and/or high pressure EGR, one or two turbochargers can be considered without loss of generality).

ACKNOWLEDGEMENT

The authors would like to gratefully thank Gilles Corde for his scientific support.

REFERENCES

[1] J. Chauvin, G. Corde, and N. Petit. Transient control of a Diesel engine airpath. In *American Control Conference*, 2007.

[2] J. Chauvin, G. Corde, and N. Petit. Constrained motion planning for the airpath of a Diesel HCCI engine. In *Conference on Decision and Control*, 2006.

[3] K. Swan, M. Shahbakhti, and C.R. Koch. Predicting start of combustion using a modified knock integral method for an HCCI engine. In *Proc. SAE World Congress*, number 2006-01-1086, 2006.

[4] J.C. Livengood and P.C. Wu. Correlation of auto ignition phenomena in internal combustion engines and rapid compression machine. In *Fifth International Symposium on Combustion*, pages 347–356, 1955.

[5] J. Heywood. *Internal combustion engine fundamental*. Mc Graw-Hill, Inc, 1988.

[6] F.G. Chmela and G. C. Orthaber. Rate of heat release prediction for direct injection diesel engines based on purely mixing controlled conditions. In *Proc. SAE World Congress*, number 1999-01-0186, 1999.

[7] M. Hillion, J. Chauvin, and N. Petit. Controlling the start of combustion on an HCCI diesel engine. In *American Control Conference*, 2008.

[8] G. Haraldsson, P. Tunestål, B. Johansson, and J. Hyvonen. HCCI combustion phasing with closed-loop combustion control using variable compression ratio in a multi cylinder engine. In *Proc. SAE World Congress*, number 2003-01-1830, 2003.

[9] J-O. Olsson, P. Tunestål, and B. Johansson. Closed-loop control of an HCCI engine. In *Proc. SAE World Congress*, number 2001-01-1031, 2001.

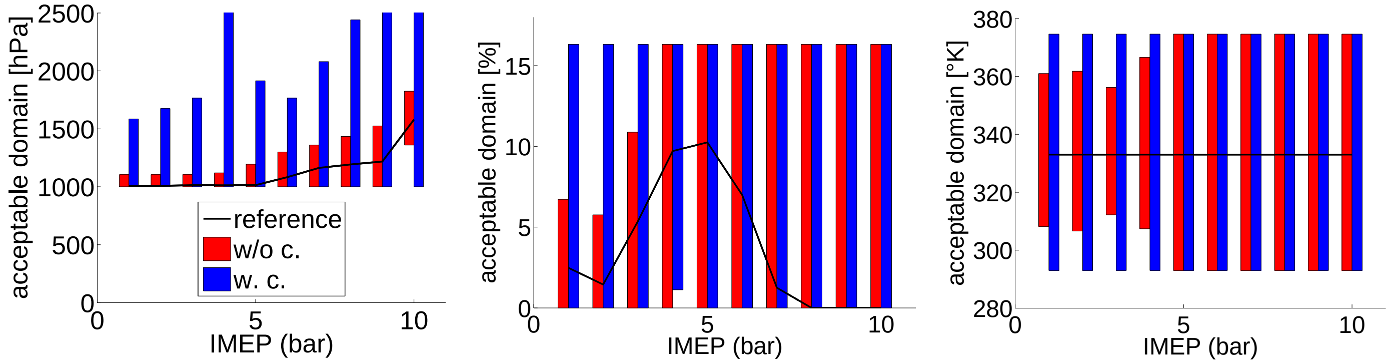

(a) Intake Manifold Pressure (b) Intake Manifold Burned Gas Rate (c) Intake Manifold Temperature

Figure 7: Acceptable domains at 800rpm, without correction (w/o c.) and with correction (w. c.).

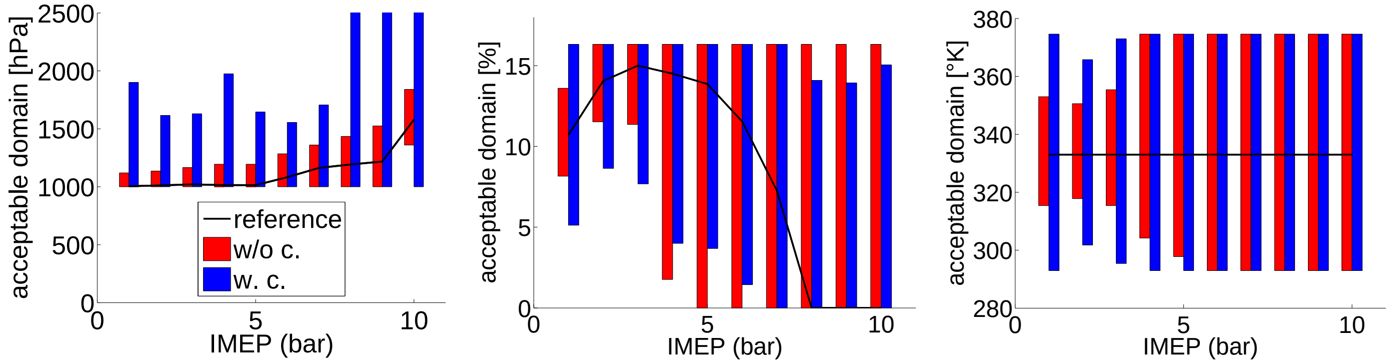

(a) Intake Manifold Pressure (b) Intake Manifold Burned Gas Rate (c) Intake Manifold Temperature

Figure 8: Acceptable domains at 1000rpm, without correction (w/o c.) and with correction (w. c.).

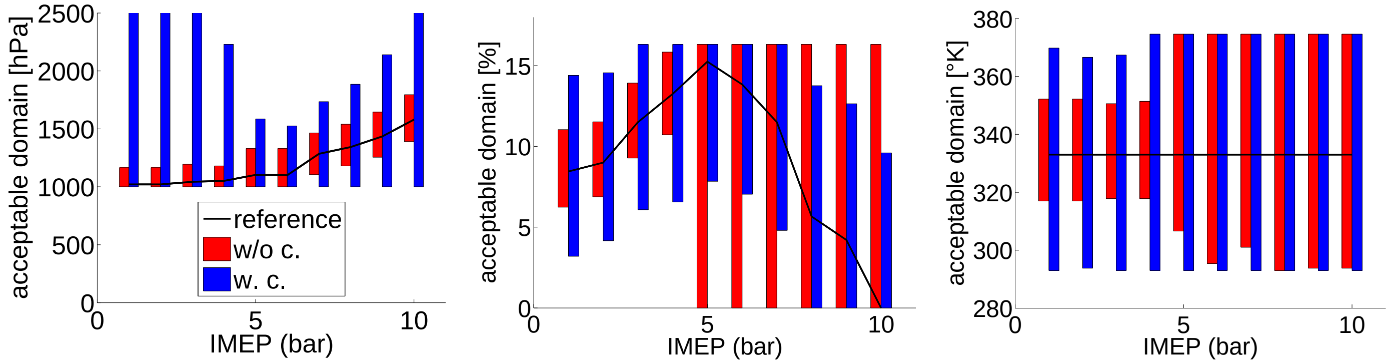

(a) Intake Manifold Pressure (b) Intake Manifold Burned Gas Rate (c) Intake Manifold Temperature

Figure 9: Acceptable domains at 1500rpm, without correction (w/o c.) and with correction (w. c.).

[10] C.J. Chiang, A. G. Stefanopoulou, and M. Jankovic. Nonlinear observer-based control of load transitions in homogeneous charge compression ignition engines. In *IEEE Transaction on Control System Technology*, volume 15, may 2007.

[11] K. Chang, G.A. Lavoie, and A. Babajimopoulos. Control of a multi-cylinder HCCI engine during transient operation by modulating residual gas fraction to compensate for wall temperature effects. In *Proc. SAE World Congress*, number 2007-01-0204, 2007.

[12] H-E. Angström, B. Eriksson, and J. Wikander. Transient control of HCCI through combined intake and exhaust valve actuation. In *Proc. SAE World Congress*, number 2003-01-3172, 2003.

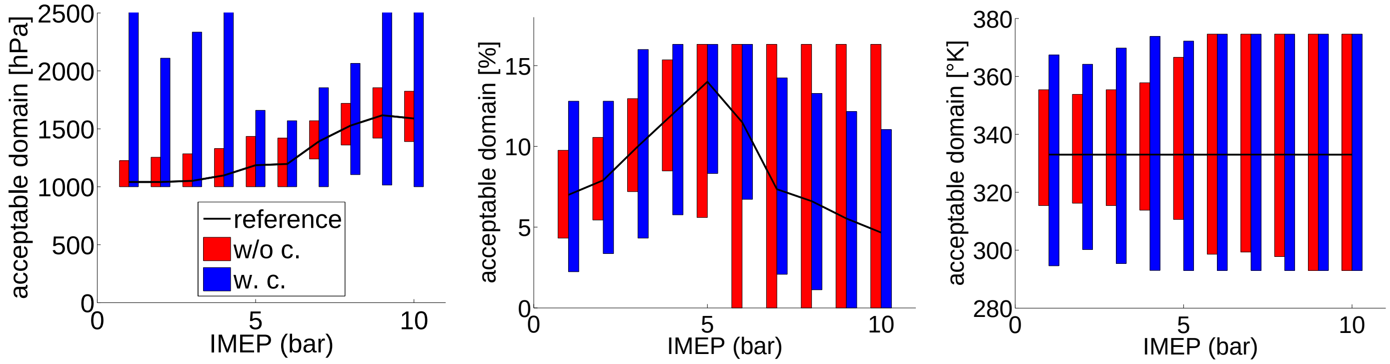

(a) Intake Manifold Pressure (b) Intake Manifold Burned Gas Rate (c) Intake Manifold Temperature

Figure 10: Acceptable domains at 2000rpm, without correction (w/o c.) and with correction (w. c.).

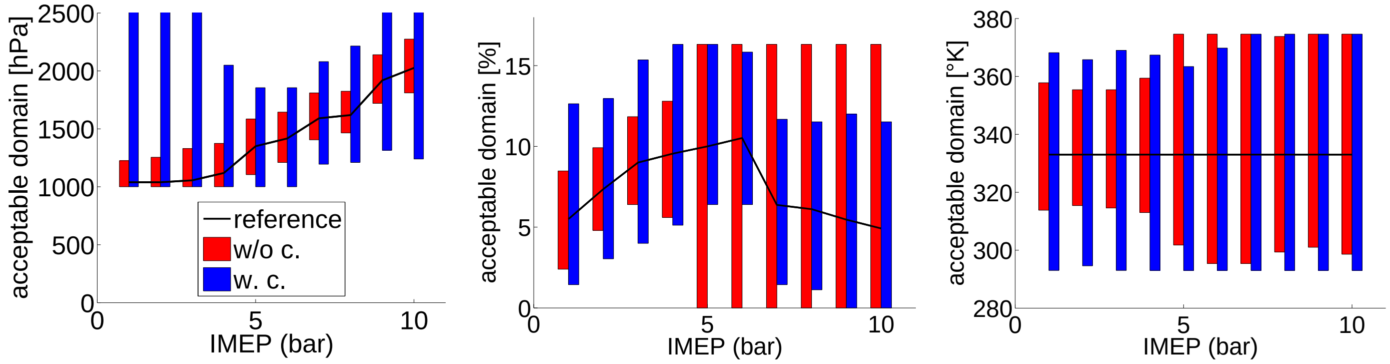

(a) Intake Manifold Pressure (b) Intake Manifold Burned Gas Rate (c) Intake Manifold Temperature

Figure 11: Acceptable domains at 2500rpm, without correction (w/o c.) and with correction (w. c.).

[13] D. Schiefer, R. Maennel, and W. Nardoni. Advantages of diesel engine control using in-cylinder pressure information for closed loop control. In *Proc. SAE World Congress*, number 2003-01-0364, 2003.

[14] C. Vigild, C.-F. Tumelaire, D. Röttger, E. Karvounis, and P.O. Calendini. Toward generic model based engine control - the concept. In *E-COSM - Rencontres Scientifiques de l'IFP*, pages 95–102, 2006.

[15] M. Hillion, J. Chauvin, and N. Petit. Active combustion control of diesel HCCI engine: Combustion timing. In *Society of Automotive Engineers*, number 2008-01-0984, 2008.

[16] C. Barba, C. Burkhardt, K. Boulouchos, and M. Bargende. A phenomenological combustion model for heat release rate prediction in high-speed di diesel engines with common rail injection. In *Proc. SAE World Congress*, number 2000-01-2933, 2000.

[17] F.-A. Lafossas, M. Marbaix, and P. Menegazzi. Development and application of a 0D D.I. Diesel combustion model for emissions prediction. In *Proc. SAE World Congress*, number 2007-01-1841, 2007.

[18] D. J. Rausen, A. G. Stefanopoulou, J-M. Kang, J. A. Eng, and T-W. Kuo. A mean-value model for control of homogeneous charge compression ignition (HCCI) engines. In *IEEE Proceedings of American Control Conference*, 2004.

[19] LMS IMAGINE. http://www.lmsintl.com/imagine.

[20] A. Albrecht, O. Grondin, F Le Berr, and Le Solliec G. Towards a stronger simulation support for engine control design: a methodological point of view. In *ECOSM, rencontres scientifiques de l'IFP.*, 2006.